Modeling $\delta^{18}O$ in precipitation over the tropical Americas: 2. Simulation of the stable isotope signal in Andean ice cores

M. Vuille,[1] R. S. Bradley,[1] R. Healy,[2] M. Werner,[3] D. R. Hardy,[1] L. G. Thompson,[4] and F. Keimig[1]

[1]   We use the ECHAM-4 and the GISS II atmospheric general circulation models (AGCM) with incorporated stable isotopic tracers and forced with observed global sea surface temperatures (SST) between 1979 and 1998, to simulate the $\delta^{18}O$ signal in three tropical Andean ice cores, from Huascarán (Peru), Quelccaya (Peru), and Sajama (Bolivia). In both models, the simulated stable isotopic records compare favorably with the observational data, when the seasonality of precipitation and dry season loss due to sublimation and wind scour are taken into account. Our simulations indicate a significant influence of the local climatic conditions (temperature and precipitation amount) on the $\delta^{18}O$ signal. Moisture source variability appears to be less of a factor on interannual timescales. Even though the moisture originates over the Amazon basin and the tropical Atlantic, correlation fields with National Centers for Environmental Prediction-National Center for Atmospheric Research (NCEP-NCAR) Reanalysis atmospheric variables and SST data indicate a dominant tropical Pacific control on interannual timescales. More enriched (depleted) $\delta^{18}O$ values are associated with periods of warm (cold) conditions in the tropical Pacific. This is consistent with modern observational evidence, which shows that climate and atmospheric circulation in the tropical Andes are closely correlated with SST anomalies in the tropical Pacific domain on interannual to interdecadal timescales. The growing number of stable isotope records from tropical Andean ice cores may thus provide an important archive for reconstructing Pacific climate variability.   *INDEX TERMS:* 1620 Global Change: Climate dynamics (3309); 1863 Hydrology: Snow and ice (1827); 4215 Oceanography: General: Climate and interannual variability (3309); 4522 Oceanography: Physical: El Niño; 9360 Information Related to Geographic Region: South America; *KEYWORDS:* GCM (general circulation model), ice cores, stable isotopes, Andes, ENSO, sea surface temperature (SST)

1.   Introduction

[2]   Over the last two decades, an increasingly dense network of tropical and subtropical ice core records has been established along the Andes of South America (Figure 1). Two records from Peru (Quelccaya, 13°56′S, 70°50′W and Huascarán, 9°S, 77°30′W) and one from Bolivia (Sajama, 18°06′, 68°53′W) have been published so far [*Thompson et al.*, 1985, 1995, 1998]. Further work is in progress on three additional ice cores recovered more recently from Illimani (16°37′S, 67°46′W) in Bolivia [*Wagnon et al.*, 2001; *Hoff-*

mann et al., 2002; E. Ramirez et al., A new Andean deep ice core from the Illimani (6350 m), Bolivia, submitted to *Earth and Planetary Science Letters.*, 2002], Cerro Tapado (30°08′S, 69°55′W) in subtropical Chile [*Stichler et al.*, 2001; *Ginot et al.*, 2001] and from Chimborazo (1°30′S, 78°36′W) in Ecuador (B. Francou, personal communication, 2001).

[3]   In the past, the $\delta^{18}O$ signal preserved in the ice has usually been interpreted as a proxy for temperature [e.g., *Thompson et al.*, 2000], but more recently this interpretation has been challenged and the stable isotopic composition has been used as an indicator for wet or dry conditions in the central Andes [e.g., *Baker et al.*, 2001]. Unfortunately, very little is known about the modern and past climate-stable isotope relationship in this part of the world, although efforts are under way to establish better knowledge of how the $\delta^{18}O$ composition of modern snowfall relates to climate at the site [*Vuille et al.*, 1998; *Hardy et al.*, 1998, D. R. Hardy et al., manuscript in preparation, 2003] (hereinafter referred to as Hardy et al., manuscript in preparation, 2003). The few observational studies that have

---
[1]Climate System Research Center, Department of Geosciences, University of Massachusetts, Amherst, Massachusetts, USA.
[2]Woods Hole Oceanographic Institution, Woods Hole, Massachusetts, USA.
[3]Max Planck Institute for Biogeochemistry, Jena, Germany.
[4]Byrd Polar Research Center, Ohio State University, Columbus, Ohio, USA.
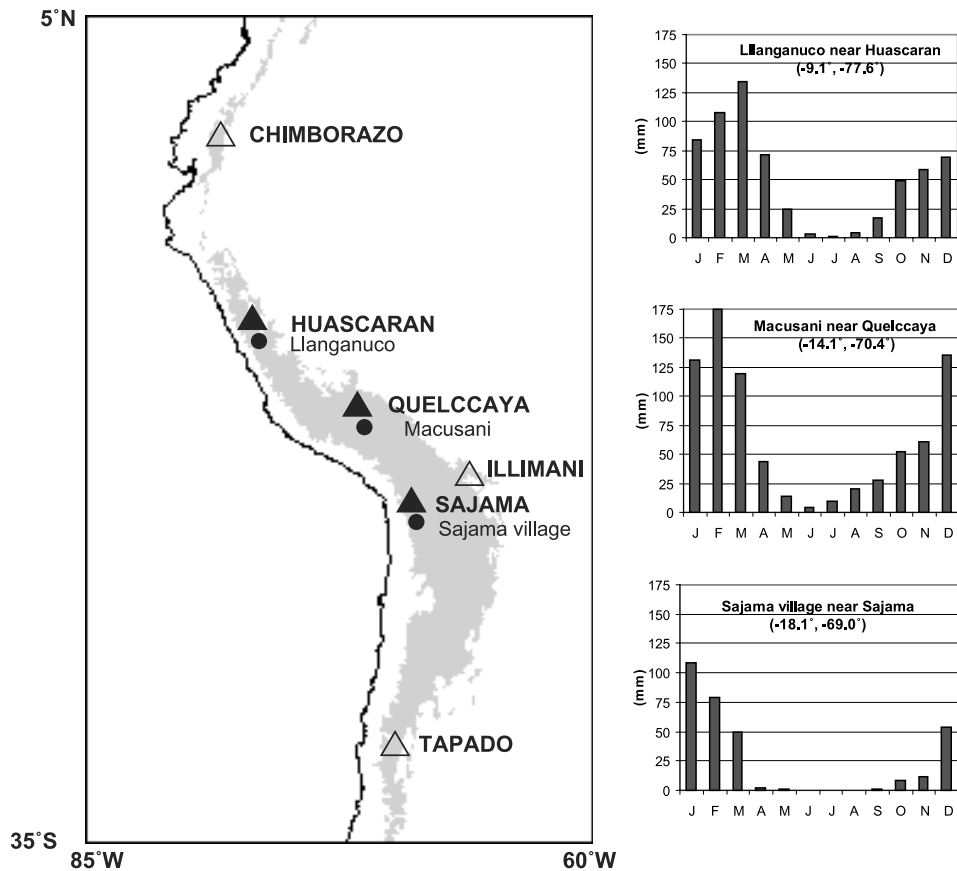
Figure 1. Map indicating tropical Andean ice core drilling sites. Black triangles show locations, which are the focus of this study. Black dots indicate precipitation records, closest to ice core locations. Seasonality of precipitation (monthly long-term mean) at these stations is shown to the right.

been pursued in the Andes [e.g., *Chaffaut et al.*, 1998; *Garcia et al.*, 1998; *Aravena et al.*, 1999; *Gonfiantini et al.*, 2001] have shed some light on the climatic controls on $\delta^{18}O$ variability, but they are too limited both in space and time to be applicable in the interpretation of Andean ice core records.

[4] Most attempts to interpret the stable isotope composition of tropical Andean ice cores have relied on Rayleigh-type distillation models, tracing the $\delta^{18}O$ signal back to its moisture source in the tropical Atlantic. *Grootes et al.* [1989] were the first to use such a model and were able to explain the strong depletion and seasonality of $\delta^{18}O$ seen in the Quelccaya record. They showed that the depletion is caused by a combination of a continentality and an altitude effect, and that seasonal variations in the $\delta^{18}O$ ratio are due to depletion of the air masses along their transport over the Amazon basin during the rainy season only. The seasonal signal is further amplified by sublimation of snow on the surface, which causes an enrichment of the surface layer. Although the general mechanism presented by *Grootes et al.* [1989] is correct, new evidence indicates that some of their assumptions need to be reassessed. Both observational evidence and model results show that air masses moving inland over the Amazon basin are depleted in heavy isotopes both in the wet and dry seasons, although the continental gradient is less during the drier period of the year [*Vuille et al.*, 2003]. Recent studies on the influence of

sublimation on stable isotope records recovered from subtropical ice cores indicate that enrichment does indeed occur, but that most of the enriched layer is actually removed from the snow surface during the sublimation process [*Stichler et al.*, 2001].

[5] *Pierrehumbert* [1999] also used a simple Rayleigh distillation model to reinterpret the $\delta^{18}O$ record from Huascarán during the last glacial maximum (LGM) and showed that the strong depletion in stable isotopes at that time can be explained by stronger rainout of the air masses over the tropical continent. The observed low LGM $\delta^{18}O$ values thus do not necessarily demand a cooling of $8°-12°C$; a temperature reduction that would be inconsistent with the $4°-6°C$ cooling inferred from snow line reconstructions [e.g., *Rind and Peteet*, 1985].

[6] Another approach to interpret the Quelccaya ice core record was proposed by *Melice and Roucou* [1998], who used a singular spectrum analysis and the wavelet transformation technique to relate the $\delta^{18}O$ record to global sea surface temperatures (SST). In their study, *Melice and Roucou* [1998] found a close correlation between the Quelccaya $\delta^{18}O$ signal and SST in the tropical North Atlantic, which would indicate that the stable isotope composition on Quelccaya is rather an indicator of climate variability in the moisture source region and does not primarily reflect climate variability in the central Andes itself. On the other hand, they also found a close correla-

tion between the Quelccaya $\delta^{18}O$ record and lake level fluctuations of nearby Lake Titicaca, which would rather argue for a tropical Pacific signal in the $\delta^{18}O$ record of Quelccaya, since fluctuations of the Titicaca lake level are largely governed by ENSO [e.g., *Aceituno and Garreaud*, 1995].

[7] *Henderson et al.* [1999] used quasi-monthly $\delta^{18}O$ values over 68 years from Huascarán and concluded that the spatial distribution of SST in the western tropical Atlantic influences the 500-hPa circulation and hence the isotopic fractionation of moisture advected across tropical America. Unfortunately, their subdivision into equal monthly bins, assuming a constant accumulation rate throughout the year, leads to a bias in their $\delta^{18}O$ record toward the dry season. As shown in Figure 1, precipitation on Huascarán has a distinct seasonal cycle with a pronounced rainy and dry season. The closest nearby weather station, Llanganuco, situated only a few kilometers from the drill site at 3800 m a.s.l., indicates that 91.8% of the annual precipitation falls within the 7 months between October and April (average between 1952 and 1998). Even though the absolute amount of rainfall may be substantially different between the drill sites on Huascarán and the nearby weather station, situated more than 2000 m below, it is plausible to assume that the seasonality is identical at the two sites. Assuming a uniform rate of precipitation thus neglects the fact that the recorded $\delta^{18}O$ values reflect rainy season conditions only (minus the fraction of the snow which is lost through wind scour and sublimation in the dry season). Interpreting the record in terms of annual mean climate thus leads to a substantial bias in the interpretation of the $\delta^{18}O$ record [*Steig et al.*, 1994; *Krinner et al.*, 1997; *Werner et al.*, 2000].

[8] On a global scale, AGCMs with isotopic tracers and tagging capabilities have significantly advanced our understanding of the climate-stable isotope relationship [e.g., *Jouzel et al.*, 1996, 2000; *Hoffmann and Heimann*, 1997; *Hoffmann et al.*, 1998, 2000; *Cole et al.*, 1999]. The major advantage of AGCM simulations over conventional methods is that all factors influencing the fractionation process are explicitly parameterized, which allows testing of their relative importance. To realistically simulate the climate and spatiotemporal distribution of $\delta^{18}O$ in the tropical Andes, however, provides a particular challenge because of the high topography and its influence on precipitation, temperature, and atmospheric circulation.

[9] In a companion paper, *Vuille et al.* [2003] provide evidence that the ECHAM-4 and GISS II GCMs are able to realistically portray the climate and the $\delta^{18}O$ distribution over the tropical Americas. Here we use the high-resolution (T106) version of the ECHAM-4 model and the GISS II model with improved topographic control over the Andes [*Vuille et al.*, 2003] to simulate the $\delta^{18}O$ composition of the three tropical Andean ice cores, Huascarán, Quelccaya, and Sajama over the last 20 years. In the next section, we describe the two simulation experiments and provide further evidence that they are capable of accurately portraying the climate of the Andes. In section 3, the simulated stable isotope records are compared with their observational counterparts and in section 4 they are tested for the relative influence of temperature, precipitation amount, moisture source variability, and atmospheric circulation (ENSO).

Section 5 provides a discussion of the results and ends with some concluding remarks.

2. Model Experiments and Performance

[10] Comparing results from AGCM simulations with ice core data is particularly problematic in the case of tropical ice cores, all drilled at high-elevation sites (>5000 m). Our GISS II simulation is therefore based on a new version of the model, which includes nine vertical levels, a higher spatial resolution (4°lat × 5°long), and an Andean topography, which has been raised to the 90th percentile (that is, the elevation at which 90% (10%) of the area within each 4° × 5° grid cell lies below (above) this level). The ECHAM-4 isotope model is based on 19 vertical layers and was run with T106 spectral resolution (~1.1°lat × 1.1°long), which is currently the highest resolution AGCM available incorporating stable isotope tracers. Both models were run with modern boundary conditions, as described in the work of *Vuille et al.* [2003]. The time periods of integration are 18 years for the GISS II model (1980–1997) and 20 years for the ECHAM-4 model (1979–1998). The first year in both simulations was discarded to avoid data problems with model equilibration during spin-up time. The GISS II simulation includes tagging capabilities; thus, water molecules precipitating over Huascarán, Quelccaya, and Sajama can be traced back to their evaporative source area. This allows us to determine the relative contribution of different source regions (see Figure 1 in the work of *Vuille et al.* [2003]) to precipitation and to assess the $\delta^{18}O$ signature of the different source regions at the three sites.

[11] *Vuille et al.* [2003] showed that both models accurately portray the essential features of surface climate over the tropical Americas in terms of both their spatial and temporal characteristics. We therefore limit the analysis of model performance to the most important anomaly fields, which we compare with observational evidence from NCEP-NCAR reanalysis data [*Kalnay et al.*, 1996] in Figure 2. The time versus longitude sections in Figure 2 are zonally averaged between ~5°N and ~10°S, from ~90°W (eastern tropical Pacific) across the Andes to ~60°W (Amazon basin) between 1980 and 1994. The spatial and temporal variability of surface temperature is nicely reproduced in all simulations (Figure 2a), with the major El Niño (La Niña) phases in 1982/83, 1986/87, and 1991/92 (1984/85 and 1988/89) standing out prominently as positive (negative) anomalies in both observations and model experiments. The temporal persistence of both positive and negative anomalies is accurately reproduced in both simulations. The major ENSO-related anomalies are also reproduced in the simulated precipitation fields (Figure 2b) although the ECHAM-4 model lacks some of the temporal persistence observed in the NCEP-NCAR reanalysis data. The GISS II simulation on the other hand has certain difficulties in simulating the observed east-west differentiation with stronger amplitude over the eastern tropical Pacific than over the Amazon basin. This is most likely a result of the coarser resolution, because the problem is not as apparent in the high resolution ECHAM-4 T106 experiment. The upper-air circulation (Figure 2c) is a crucial component of Andean climate because it is considered to be the main forcing mechanism behind wet and dry conditions [e.g., *Garreaud et al.*, 2003]. The NCEP-NCAR
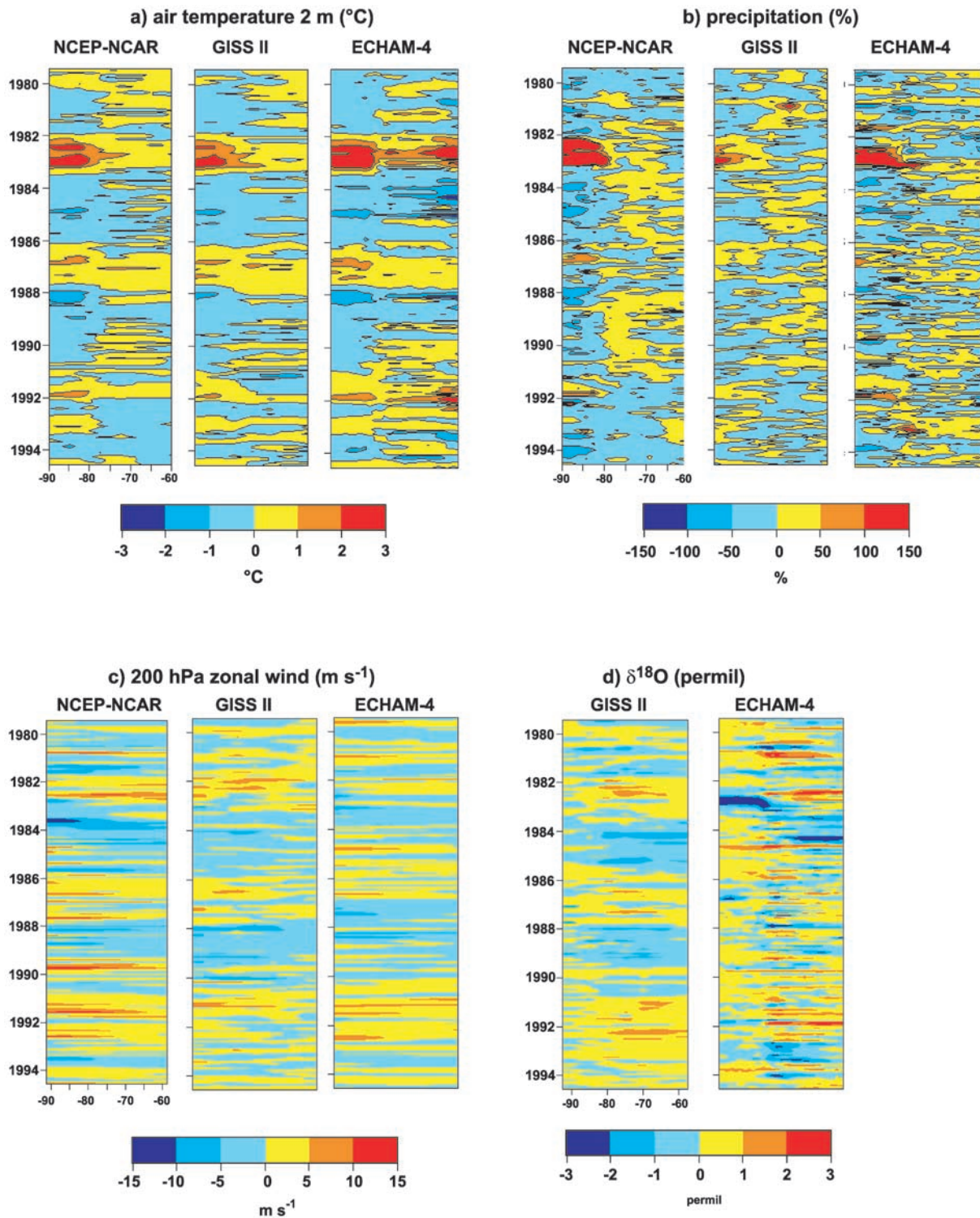
Figure 2. Time versus longitude sections of monthly anomalies of (a) surface temperature (°C), (b) precipitation (%), (c) 200 hPa zonal wind (m s^{-1}), and (d) δ^{18}O of precipitation (‰) between 1980 and 1994. Shown from left to right are results for NCEP-NCAR reanalysis, GISS II, and ECHAM-4 T 106, except for Figure 2d where only model results are shown. Reference period for anomalies is 1980–1994. Analyses are based on zonal average between ~5°N and ~10°S and show cross-section through the tropical Andes from ~90°W (eastern tropical Pacific) to ~60°W (Amazon basin). Latitudinal and longitudinal extent varies slightly between reanalysis and the different models due to different grid cell sizes.

200 hPa zonal wind anomalies reflect the major ENSO periods, featuring westerly (easterly) flow during El Niño (La Niña) phases (compare Figures 2a and 2c), which is correctly simulated by both models. Finally, Figure 2d shows the simulation of the $\delta^{18}O$ anomalies of precipitation. Here the results are clearly quite different between the two models. The GISS II experiment shows a dominant low-frequency mode associated with ENSO, that is more enriched (depleted) values occur during El Niño (La Niña) phases. The ECHAM experiment features this characteristic as well, but it does not show such a high degree of temporal persistence; the amplitude of the anomalies is larger and the ENSO signal is more spatially heterogeneous; the sign of the anomaly is not necessarily the same across the Andes from 90° to 60°W. The T106 simulation thus seems capable of more realistically portraying east-west differences in the $\delta^{18}O$ signal, such as during the 1982/1983 El Niño with more depleted (enriched) values over the Pacific (Amazon basin).

3. Simulated Ice Core Records

[12] To simulate the $\delta^{18}O$ record in the three ice cores from Huascarán, Quelccaya, and Sajama, first requires that certain grid cells in the models be assigned to each of the three records. *Werner and Heimann* [2002] in their simulation of ice core records from the Summit (Greenland) and Law Dome region (Antarctica) compared the actual data from the grid cell covering the drill site with the ice core records. While this approach seems feasible over rather homogeneous terrain, it is not appropriate over the Andes, which act as a strong climatic barrier between the humid Amazon basin and the arid Pacific coast. Because of the coarse resolution (in particular in the GISS II model), this gradient is represented by discrete steps and not as a gradual change, and the actual climate at a particular site cannot be accurately reproduced when using just one grid cell. We therefore used an inverse distance-weighted average of all grid cells within a predefined distance from the drilling location to simulate the monthly temperature, precipitation, and $\delta^{18}O$ record at the three sites: Huascarán, Quelccaya, and Sajama. Because of the very different resolution, we used a different threshold for the two models: 200 km for the ECHAM-4 simulation and 400 km for the GISS II model. That is, the simulated record at each site is the inverse distance-weighted average of all grid cells, centered within a 200 km (400 km) radius of the drill site.

[13] Except for Sajama, where we used a new monthly record of $\delta^{18}O$ (Hardy et al., manuscript in preparation, 2003), which accounts for the strong seasonality in precipitation observed on this mountain (Figure 1), only annual values of observed $\delta^{18}O$ are available. For the reasons mentioned above, we did not use the published quasi-monthly record from Huascarán [*Henderson et al.*, 1999]. In order to compare simulated and observed values, the simulated monthly $\delta^{18}O$ values thus need to be averaged into one value per year as well. As pointed out by *Steig et al.* [1994] and others, the only correct way to do this is to use a precipitation-weighted average of the monthly $\delta^{18}O$ values. This accounts for the strong seasonality of precipitation at these tropical and subtropical locations and yields the most representative annual value. However, as discussed in detail by Hardy et al. (manuscript in preparation, 2003),

Ginot et al. [2001] and *Stichler et al.* [2001], not all of the snow falling on the summit is actually retained in the ice core, but considerable amounts are lost during the dry season due to sublimation and wind scour. On Sajama, for instance, several years of detailed field measurements show that, on average, only the snow falling between the start of the rainy season (November) and February is preserved in the ice core, while all the snow falling toward the end of the rainy season (March and April) or during occasional winter snowfall episodes (May–October) is subsequently removed from the snow surface by wind scour and sublimation (Hardy et al., manuscript in preparation, 2003). This needs to be taken into account when comparing simulated with observed $\delta^{18}O$ records. The annual simulated value of $\delta^{18}O$, temperature, and precipitation on Sajama is therefore based on the precipitation-weighted mean between November and February only. These four months account for 80.2% of the annual precipitation total in Sajama village (Figure 1). On Huascarán and Quelccaya unfortunately, such detailed information from field campaigns is not available. However, it is likely that wind scour and sublimation are considerably lower in those tropical locations than on Sajama, located in the dry subtropics. In addition, the rainy season is spread out over a longer time period, starting in October and lasting into April (see Figure 1). We thus decided to use those seven rainy season months for our simulation. Since we still use a precipitation-weighted average and the nearby precipitation records indicate that the months from October until April account for 90.4% (91.8%) of the annual precipitation falling on Quelccaya (Huascarán); using all 12 months would make little difference.

[14] The comparison of our simulated $\delta^{18}O$ records with the ice core (observational) data in Figure 3 is an additional indication that it is indeed the rainy season signal only which is preserved in the ice core records, as suggested by Hardy et al. (manuscript in preparation, 2003). Because of the high-altitude location of the drill sites, the values in our simulations are considerably more enriched and not directly equivalent with those measured in the ice cores. We therefore use standardized anomalies to compare the simulated interannual variability with the observational ice core record.

[15] Unfortunately, the original Quelccaya record ends in 1984 [*Thompson et al.*, 1985] and more recent data is affected by percolation of meltwater, destroying the original $\delta^{18}O$ signal [*Thompson et al.*, 1993]. The 4 (5) years of overlap between the observed and simulated record by the GISS II (ECHAM-4) model do not allow an evaluation of their performance. On Huascarán and Sajama, however, there is a clear coherence between observed and simulated records. On Sajama, the correlation between observed and simulated annual $\delta^{18}O$ value is 0.72 (0.68) for the ECHAM-4 (GISS II) model, significant at the 99.9% (99%) level. On Huascarán, the correlation is 0.49 (0.65), for the ECHAM-4 (GISS II) model, which is lower than on Sajama, but still significant at the 90% (95%) level. The performance of the two models is further put into perspective by considering that the correlation between the core on Huascarán and a second core drilled at the same location is only 0.82 over this same time interval. The fact that both models are able to quite accurately simulate the interannual variability of $\delta^{18}O$ at these high tropical locations should by no means be taken for granted. For example, *Werner and Heimann* [2002]
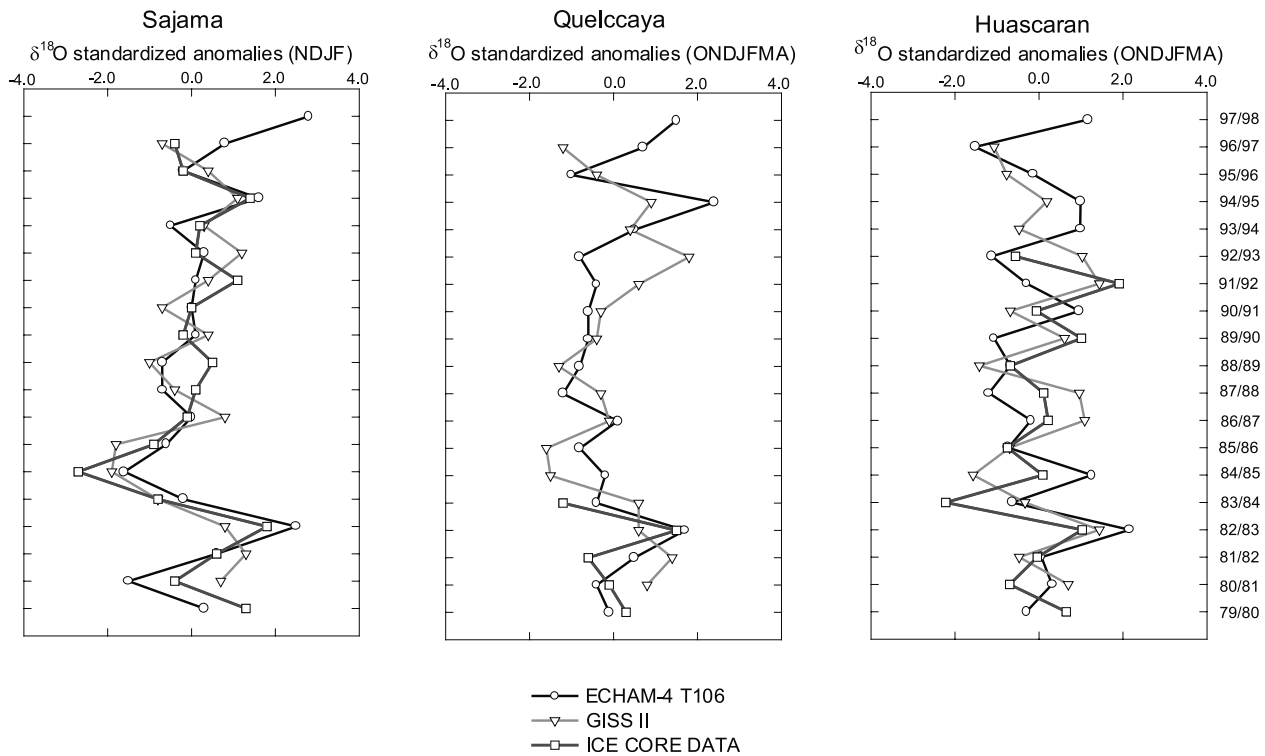
Figure 3.   Observed versus simulated interannual variability of $\delta^{18}O$ in ice cores from Sajama (left), Quelccaya (middle), and Huascarán (right) between 1979 and 1998. Values of $\delta^{18}O$ are shown as standardized anomalies based on period 1979–1998.

showed that the ECHAM-4 model, although run with a lower spectral resolution (T30), was unable to reproduce the observed interannual variability of $\delta^{18}O$ in ice cores from Summit, Greenland. This discrepancy between the two studies occurs because the climate and $\delta^{18}O$ in the tropical Andes is largely governed by the interannual variability in the global SST-field, explicitly prescribed in the model. In Greenland, on the other hand, the simulated year-to-year variability of $\delta^{18}O$ is solely due to the stochastic internal variability of the atmosphere in the high northern latitudes and not due to the prescribed SST [*Werner and Heimann*, 2002]. This imprint of global SST on the $\delta^{18}O$ record in both observations and model simulations is a characteristic of tropical ice cores and shows their potential for climate studies on interannual timescales, in particular ENSO [e.g., *Thompson et al.*, 1984; *Thompson*, 1993; *Diaz and Pulwarty*, 1994]. The good match between simulated and observed $\delta^{18}O$ records on Sajama and Huascarán also provides proof that our approach of using precipitation-weighted annual values and discarding the precipitation during the dry season months was correct. To illustrate this, we also computed an annual record based on a simple average of 12 monthly values between July and June, as suggested in the work of *Henderson et al.* [1999]. While the correlation between this simulated record and observations is only slightly lower in the GISS model (0.63 on Sajama and 0.53 on Huascarán), it
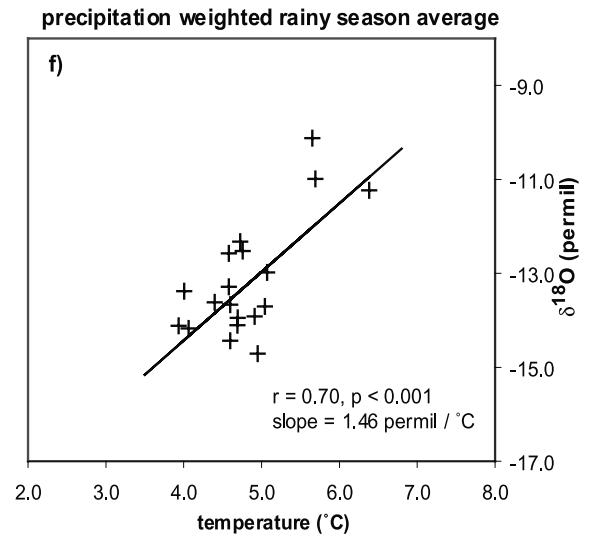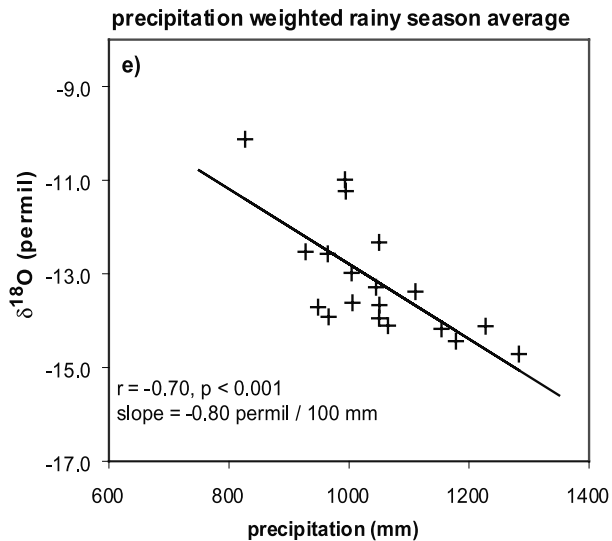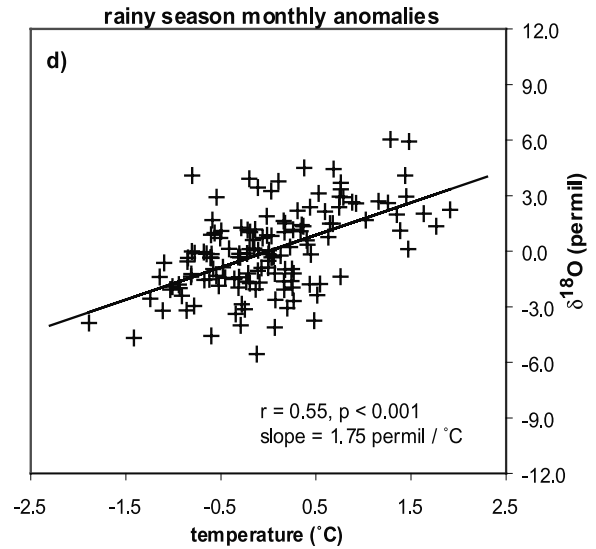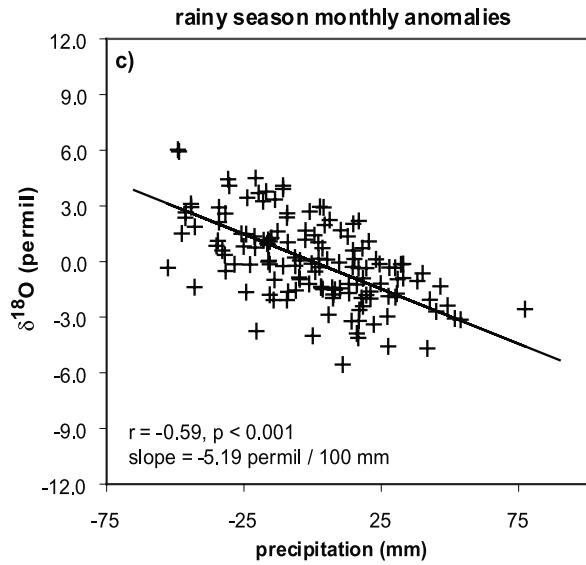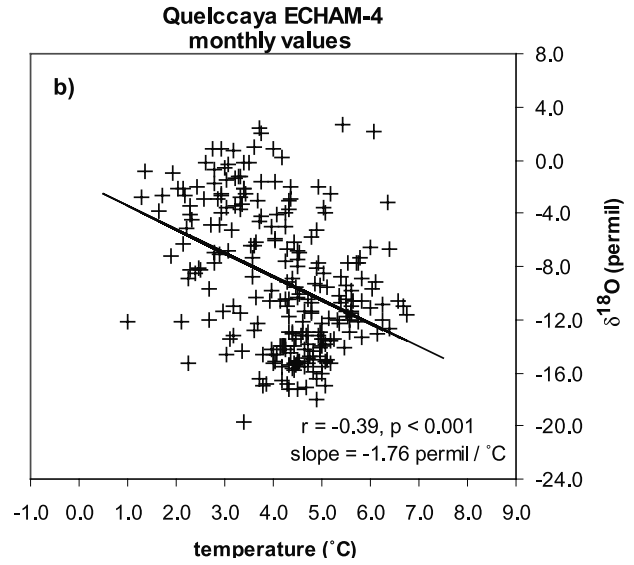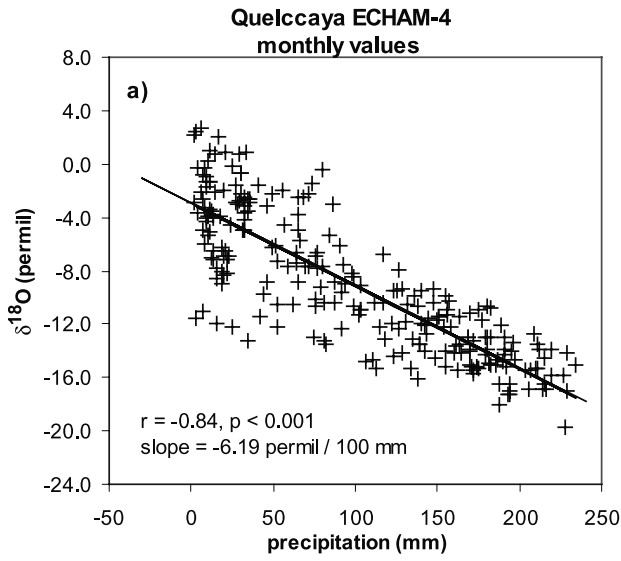
falls completely apart in the ECHAM-4 model (−0.10 on Sajama and −0.08 on Huascarán). The strong temporal persistence of the $\delta^{18}O$ anomalies in the GISS II model (see Figure 2d) leads to a very similar interannual variability, no matter how the annual $\delta^{18}O$ value is calculated. In the ECHAM-4 simulation, however, featuring a much larger intraseasonal variability, it makes a big difference whether one uses a precipitation-weighted rainy season value or a simple 12-month average.

4.   Climatic Controls on $\delta^{18}O$

4.1.   Temperature and Precipitation Amount

[16]   Since both models seem capable of quite accurately portraying the interannual variability of $\delta^{18}O$ in tropical Andean ice cores, we next discuss the influence of local climatic parameters (surface temperature and precipitation amount) on the $\delta^{18}O$ records at timescales ranging from monthly to interannual. We emphasize the issue of different timescales because it has been argued that the observed negative relationship between monthly $\delta^{18}O$ composition of precipitation and temperature at low latitudes may fall apart or change sign on longer timescales [*Thompson et al.*, 2000]. The evidence based on our model simulations indeed points in this direction for the $\delta^{18}O$-temperature relationship. As shown in Figure 4b, on Quelccaya, the ECHAM-4 model

Figure 4.   (opposite) Scatterplots of simulated $\delta^{18}O$ of precipitation versus precipitation amount (left column) and surface temperature (right column) in Quelccaya ice core based on ECHAM-4 (1979–1998) simulation. (a–b) Correlation and slope of monthly values. (c–d) Correlation and slope of monthly rainy season anomalies (October–April only). (e–f) Correlation and slope of annual precipitation-weighted rainy season average.

Quelccaya ECHAM-4
monthly values

a)

r = -0.84, p < 0.001
slope = -6.19 permil / 100 mm

Quelccaya ECHAM-4
monthly values

b)

r = -0.39, p < 0.001
slope = -1.76 permil / ˚C

rainy season monthly anomalies

c)

r = -0.59, p < 0.001
slope = -5.19 permil / 100 mm

rainy season monthly anomalies

d)

r = 0.55, p < 0.001
slope = 1.75 permil / ˚C

precipitation weighted rainy season average

e)

r = -0.70, p < 0.001
slope = -0.80 permil / 100 mm

precipitation weighted rainy season average

f)

r = 0.70, p < 0.001
slope = 1.46 permil / ˚C

Table 1. Correlation Coefficients in ECHAM-4 and GISS II Simulations Between Dependent Variable Rainy Season $\delta^{18}O$ and Independent Variables Precipitation Amount, Surface Temperature, NINO3.4 Index, and Source Contributions (for GISS II Experiment and Source Contributions >2% Only)[a]

	Precipitation Amount	Surface Temperature	NINO3.4	Equatorial Pacific	Tropical South America	Equatorial Atlantic	Subtropical South America	Tropical South Atlantic	Multiple r
ECHAM-4									
Sajama	−0.66[b]	**0.87**[b]	0.73[b]	. . .	. . .	. . .	. . .	. . .	0.87
Quelccaya	−**0.70**[b]	**0.70**[b]	0.56[c]	. . .	. . .	. . .	. . .	. . .	0.81
Huascarán	0.20	**0.51**[c]	0.39	. . .	. . .	. . .	. . .	. . .	0.51
GISS II									
Sajama	−**0.45**	0.41	**0.57**[c]	. . .	0.12	0.23	−0.25	−0.02	0.74
Quelccaya	−**0.52**[c]	0.39	**0.50**[c]	. . .	−0.44	0.07	−0.19	**0.52**[c]	0.72
Huascarán	0.02	0.68[b]	**0.83**[b]	−0.43	−0.35	0.41	. . .	0.20	0.83

[a]Both dependent and independent variables are weighted by the monthly precipitation amount between October and April (Huascarán and Quelccaya) and between November and February (Sajama), respectively. Bold numbers indicate that variable enters a backward stepwise multiple regression model (multiple r shown in last column).
[b]Correlation significant at the 99% confidence level.
[c]Correlation significant at the 95% confidence level.

simulates a weak negative relationship between $\delta^{18}O$ composition of precipitation and monthly mean temperature at the site, consistent with observations [e.g., *Grootes et al.*, 1989]. However, if the seasonal cycle is removed (Figure 4d), the monthly temperature anomalies show a significant ($p < 0.001$) positive correlation with the $\delta^{18}O$ anomalies. This positive relationship is also apparent on interannual timescales, when comparing the rainy season precipitation-weighted values of $\delta^{18}O$ and temperature (Figure 4f). The results from the GISS model (not shown) are comparable to the ECHAM-simulation, featuring a similar reversal of the $\delta^{18}O$-temperature relationship from seasonal to interannual timescales, although the correlation does not reach statistical significance on Quelccaya on interannual timescales (Table 1). This apparent reversal is due to the dominant influence of precipitation on seasonal timescales. The warmest (coldest) months on Quelccaya are at the same time as the months of maximum (minimum) precipitation, thus leading to a negative $\delta^{18}O$-temperature relationship, which in reality is being dictated by the seasonality of precipitation.

[17] Indeed, as shown in Figure 4a, a similar negative slope occurs on the seasonal timescale between $\delta^{18}O$ composition and precipitation amount, with more depleted values in the rainy season months and more enriched values during the dry months. This relationship does not change if the seasonal cycle is removed and only monthly anomalies in the wet season (Figure 4c) or annual precipitation-weighted values of $\delta^{18}O$ (Figure 4e) are considered. The model still produces a significant amount effect, that is, more depleted $\delta^{18}O$ values occur in years with higher-precipitation amounts. A similar result emerges from the GISS simulation (not shown), although the correlation is more significant in the ECHAM simulation ($r = -0.70$ in ECHAM-4 versus $r = -0.52$ in the GISS II model, see Table 1). More importantly, the influence of the precipitation amount on the $\delta^{18}O$ composition of precipitation is a robust characteristic of both model simulations and apparent on all timescales.

[18] However as mentioned above, only the rainy season precipitation is deposited and retained in the ice core. It is thus the variability from one rainy season to the next, rather than seasonal cycles, which are relevant for the interpretation of the ice core $\delta^{18}O$. Accordingly, it is the relationship shown in Figures 4e and 4f, which determines the meaning

of the $\delta^{18}O$ as a paleoclimatic proxy, rather than the seasonal slope shown in Figures 4a and 4b.

[19] A similar analysis was performed for the Sajama and Huascarán data as well and the results are listed in Table 1 for comparison. Overall, the two models show similar results with a positive relationship between $\delta^{18}O$ and temperature and a negative association between $\delta^{18}O$ and precipitation amount. The only exception to this rule is Huascarán, where neither of the two simulations shows a significant amount effect. The significance of the correlation, however, varies substantially between the two models, and is generally higher in the ECHAM simulation. While the correlation between $\delta^{18}O$ and temperature is significant (95% confidence level or higher) on all mountains in the ECHAM-4 run, the correlation is insignificant on both Quelccaya and Sajama in the GISS II simulation. As shown by *Vuille et al.* [2003], the GISS II model has some difficulties in accurately portraying the interannual $\delta^{18}O$-temperature relationship over tropical South America, which may be part of the reason for the insignificant correlation coefficients in Table 1.

4.2. Moisture Source Variability

[20] Figure 5 shows the mean contribution (in percent) of various moisture sources to the total precipitation during the rainy season months (October–April) over the tropical Andes. Because the tagging capability was not implemented in the ECHAM-4 T106 simulation, we here limit the discussion to the results from the GISS II simulation. Clearly, there are two major moisture sources for precipitation over the three ice core sites: tropical South America (i.e., the Amazon basin, Figure 5b) and the equatorial Atlantic (Figure 5c). For the more southern location Sajama, there is also a significant contribution from the subtropical part of the continent (Figure 5e). On the other hand, except for a small contribution to precipitation on Huascarán, there is no moisture influx toward the continent from the tropical Pacific, which is in agreement with observational evidence [e.g., *Garreaud et al.*, 2003]. Table 2 lists the long-term mean contribution at each of the three ice core sites from the various source regions, which contribute at least 2% to the rainy season total. Note that while Figure 5 shows the average conditions for October–April; the numbers in Table 2, in the case of Sajama, are based on November–
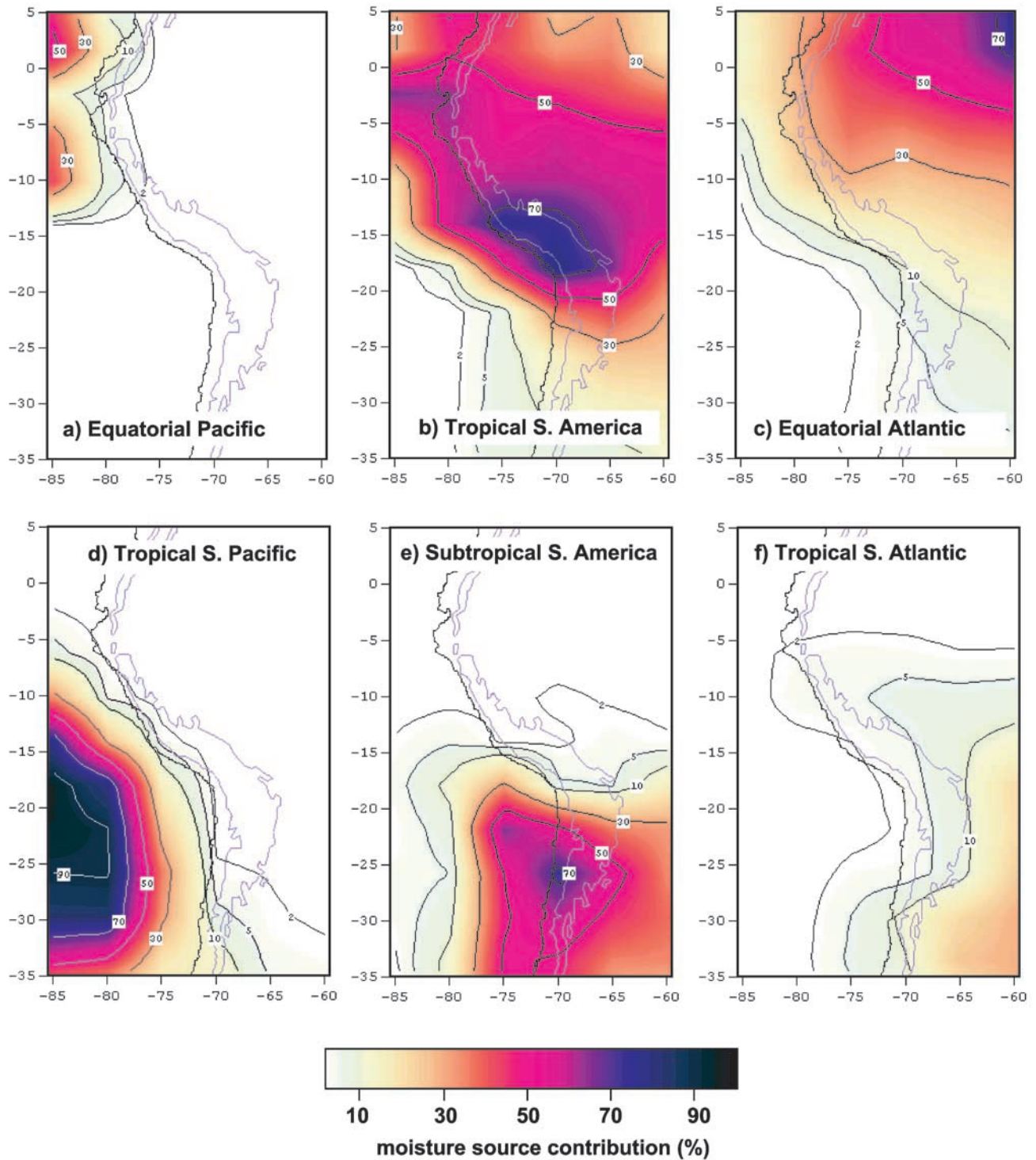
Figure 5. Simulated contribution (in percent) of source regions to precipitation in each grid cell during rainy season (October–April) between 1980 and 1997 based on GISS II model. Source regions correspond to regions as defined in Figure 1a of *Vuille et al.* [2003]: (a) equatorial Pacific, (b) tropical South America, (c) equatorial Atlantic, (d) tropical South Pacific, (e) subtropical South America, and (f) tropical South Atlantic. Contour lines indicate 2, 5, 10, 30, 50, 70, and 90% contribution.

February only. Figure 5 shows the average conditions between 1980 and 1997, but interannual variability in SSTA and the atmospheric circulation can cause a varying contribution from the different moisture sources from one year to the next. Since precipitation from each source carries a specific isotopic signature, this may cause changes in the interannual $\delta^{18}O$ composition of the ice core [e.g., *Charles et al.*, 1994; *Werner et al.*, 2001]. Figure 6 shows the time

Table 2. Simulated Contributions of Total Precipitation (±1σ) From the Six Main Moisture Sources to Precipitation at the Three Ice Cores Sites Huascarán, Quelccaya, and Sajama, Based on the GISS II Experiment[a]

Sources	Huascarán	Quelccaya	Sajama
Equatorial Pacific	3.1 ± 0.4	. . .	. . .
Tropical South America	58.8 ± 1.3	73.4 ± 1.3	69.7 ± 0.8
Equatorial Atlantic	27.7 ± 1.5	16.8 ± 1.3	10.4 ± 0.7
Tropical South Pacific	. . .	. . .	. . .
Subtropical South America	. . .	2.1 ± 0.4	14.0 ± 1.1
Tropical South Atlantic	3.6 ± 0.7	4.2 ± 0.7	3.1 ± 0.6

[a]Values are given in percent. Source contribution is based on the rainy season months whose precipitation is retained in the ice core only, that is October–April for Huascarán and Quelccaya, and November–February for Sajama, and listed only if the source contributes at least 2% to the rainy season total.

series of the simulated ice core $\delta^{18}O$ values plotted versus the percent contribution to precipitation from each source. Clearly, the simulated contribution of the different sources to precipitation at each ice core site varies little from one year to the next (see also low σ values in Table 2). Nonetheless, these variations should not a priori be ruled out as a significant contributing factor to the observed and simulated $\delta^{18}O$ signal in tropical ice cores. We thus correlated the rainy season percent contribution anomaly of each source with the simulated isotopic value of the three ice cores. The results for all three sites are listed in Table 1. As a general rule of thumb, $\delta^{18}O$ anomalies are negatively correlated with the distance from the evaporative source because of the gradual rainout and increasingly depleted composition of water vapor along its trajectory [e.g., *Cole et al.*, 1999]. Thus one might expect that the correlation between the local $\delta^{18}O$ signal in the Andes and a particular moisture source should be more negative, the farther the source is from the Andes. From Figure 6, however, no such behavior is evident, and indeed the numbers in Table 1 indicate that the influence of moisture source variability on the $\delta^{18}O$ composition seems to be very limited. Most likely this reflects the fact that the relative source contribution from one year to the next is very similar (Figure 6 and Table 2), and that more than 80% of Andean precipitation is contributed from only two source regions (Table 2). In addition, as pointed out by *Vuille et al.* [2003], the simulated long-range water vapor transport in the GISS model is rather weak. It is thus not surprising to see that only one significant relationship at the 95% confidence level emerged from our analysis, which includes the isotopic content of precipitation on Quelccaya and the percentage of Quelccaya precipitation originating over the tropical South Atlantic. However, the tropical South Atlantic, on average, contributes only 4.2% to the precipitation on Quelccaya in our GISS II simulation (Table 2), so this result should be interpreted with caution.

### 4.3. Multiple Linear Regression Analysis

[21] The different factors influencing the stable isotopic composition of precipitation are not necessarily independent from each other. On interannual timescales, the climate in the tropical Andes is either warm and dry or cold and wet, but rarely warm and wet or cold and dry. This is due to the governing influence of tropical Pacific SSTA on the atmospheric circulation over the tropical Andes, causing upper-air

zonal wind anomalies (see Figure 2c) which favor wet (dry) conditions during periods of sustained cold (warm) SSTA in the tropical Pacific [e.g., *Vuille*, 1999; *Vuille et al.*, 2000a; *Garreaud and Aceituno*, 2001; *Garreaud et al.*, 2003]. At the same time, surface temperature in the tropical Andes closely tracks SSTA in the central equatorial Pacific with a lag of 1–2 months [*Diaz and Graham*, 1996; *Vuille et al.*, 2000a, 2000b], thus air temperature in the Andes is high (low) when the tropical Pacific is warm (cold). This notion is further supported by the fact that the stable isotopic composition of all ice cores is also significantly correlated with the precipitation-weighted NINO3.4 index (SSTA averaged over 5°N–5°S; 120°W–170°W) in five out of six model experiments (Table 1).

[22] One way to further investigate this multivariate dependence of $\delta^{18}O$ is to apply a multiple linear regression analysis [e.g., *Werner and Heimann*, 2002]. We used the annual $\delta^{18}O$ values as dependent variables and all other parameters listed in Table 1 entered the regression model as independent input variables. We performed a stepwise forward selection and backward elimination procedure [e.g., *Von Storch and Zwiers*, 1999], independently for each ice core location and both model simulations. All variables, which explain a significant amount of variance in the presence of the other factors at the 95% confidence level based on an F test were retained in the model. These variables are highlighted in bold and listed together with the multiple correlation coefficient of the regression model in Table 1. Our results indicate a strong autocorrelation among the independent variables with only one or two variables remaining in the model in five out of the six cases (Table 1). In particular, temperature does not significantly contribute to the model in combination with precipitation amount or the NINO3.4-index, and in only one case (Quelccaya, ECHAM-4) enters the model together with one of the other two variables. However, overall temperature is the dominant independent variable in the ECHAM simulations, while the NINO3.4-index is retained in all of the GISS experiments. The good performance of the regression models based on only a few independent variables is documented in Figure 7, where the simulated $\delta^{18}O$ records are plotted versus the multilinear fit time series. Except for the case of Huascarán in the ECHAM-4 simulation, all multiple regression models explain more than 50% of the variance.

4.4. Principal Component Analysis

[23] Another way to search for the dominant controls on the $\delta^{18}O$ composition in these tropical Andean ice cores is to extract the primary mode of common variance and to see whether this mode can be associated with any kind of physical forcing. We thus next performed a principal component analysis (PCA) in the spatial sense, using the intercore correlation matrix of the three ice cores. This analysis was done separately for the two simulations and the observational ice core $\delta^{18}O$ from the three sites. Since the common period of observational ice core data ends in 1984, we performed two PCA on the observational record for two different time periods: 1976–1984 and 1964–1984. The first period is very short but is entirely based on data after the 1976 Pacific climate shift [e.g., *Ebbesmeyer et al.*, 1991; *Stephens et al.*, 2001], similar to the simulated
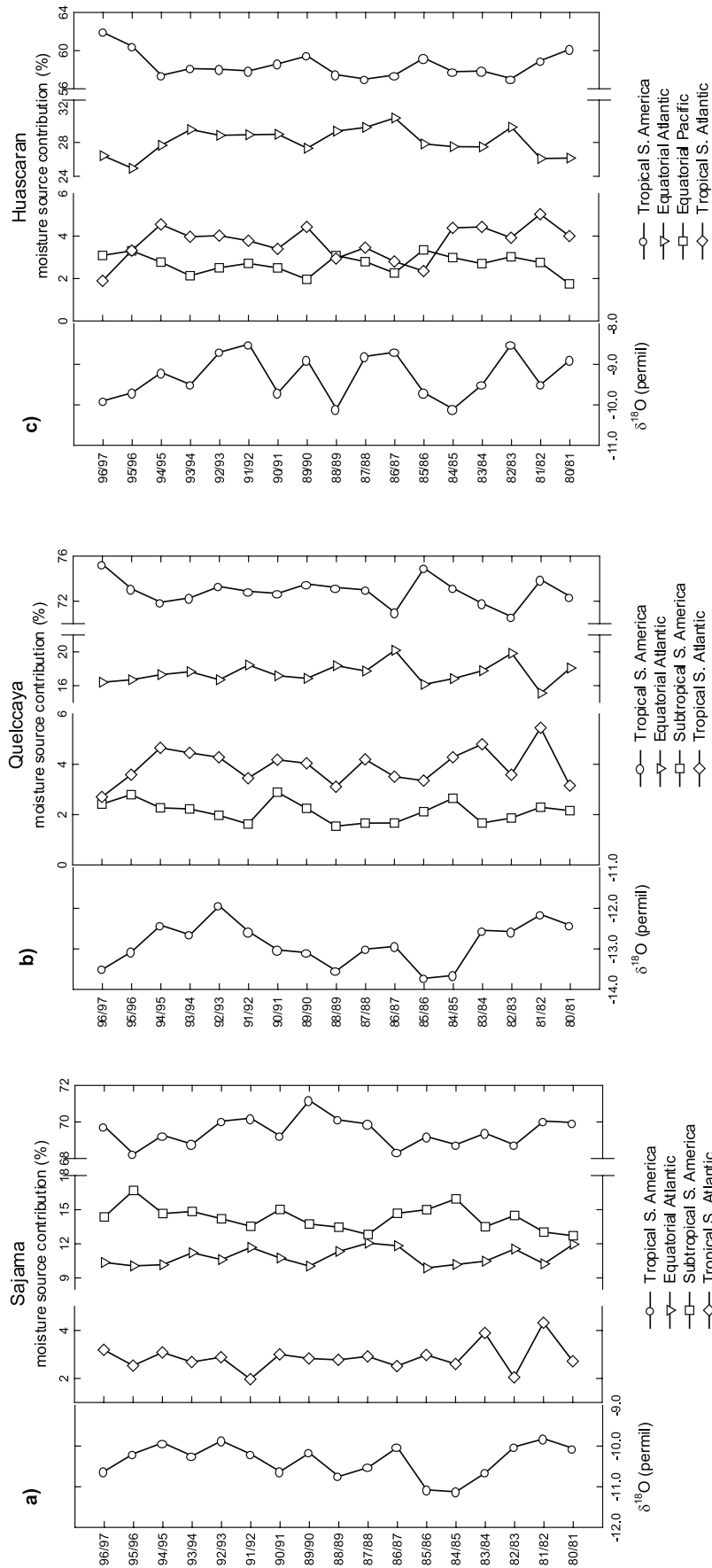
Figure 6. Simulated precipitation-weighted rainy season average of $\delta^{18}O$ in precipitation and percent contribution of each source in the GISS II model for: (a) Sajama, (b) Quelccaya, and (c) Huascarán. Moisture source contributions are only plotted for source regions that contribute at least 2‰ to the total rainy season precipitation. Note breaks in scaling of moisture source contribution.
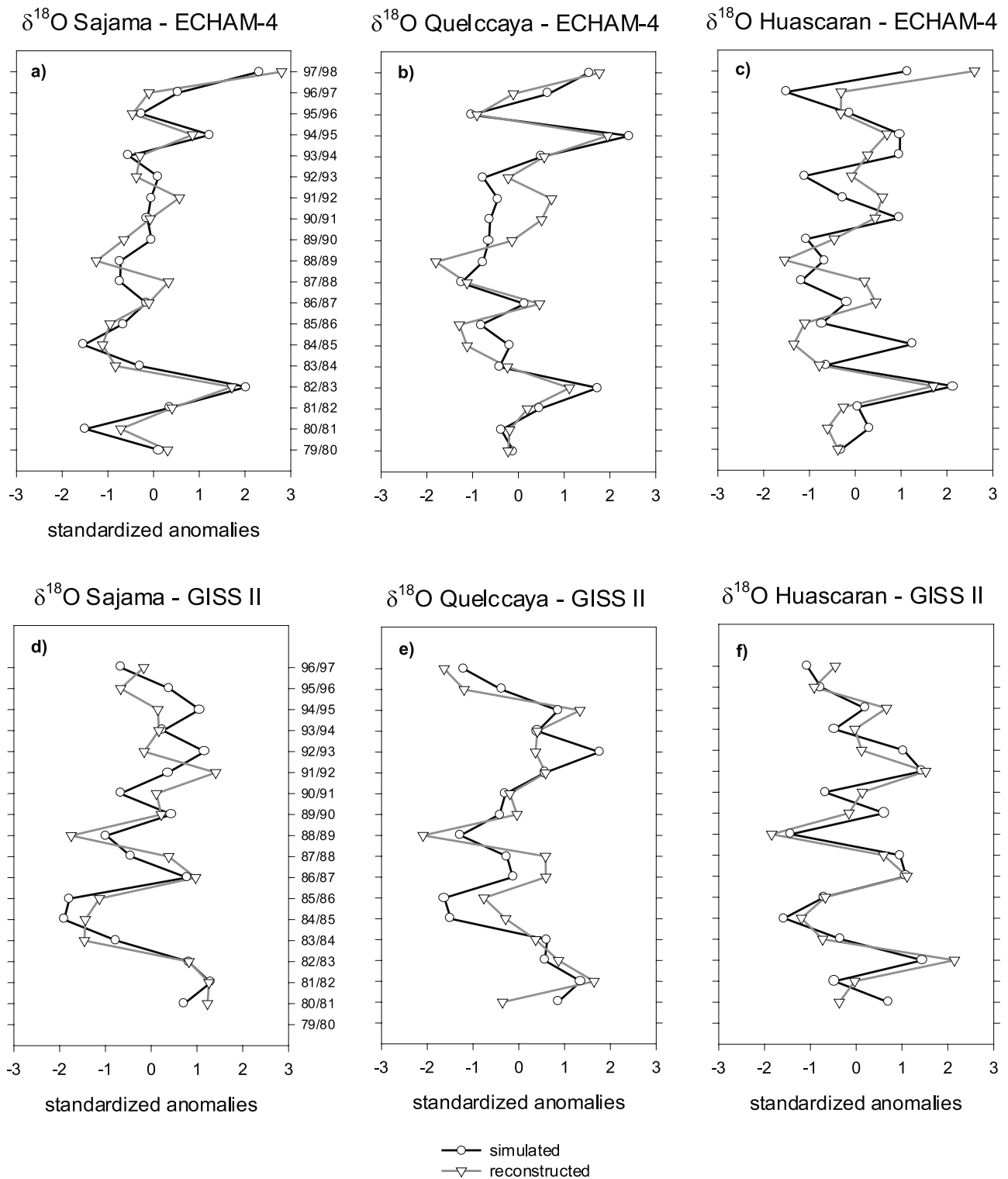
Figure 7. Simulated precipitation-weighted rainy season average of $\delta^{18}O$ records (standardized anomalies) versus multilinear fit on Sajama (left column), Quelccaya (middle column), and Huascarán (right column) based on ECHAM-4 (top row) and GISS II (bottom row). Time series of the multilinear fits are based on multiple regression analysis using the predictors as defined in Table 1.

records (GISS II: 1980–1997, ECHAM-4: 1979–1998), while the second time period covers an equal length of time as the PCs from the simulated ice cores (~20 years) but goes back to before the Pacific climate shift. In each

case, we limit our interpretation to the PC#1, since the other two explain very little of the total variance and most likely are not associated with anything really physically meaningful. Table 3 lists the percent of total explained variance

Table 3. Percent of Total Explained Variance and Factor Loadings of PC#1 of Annual $\delta^{18}O$ From Tropical Ice Cores Based on Observations (Ice Core Data) and Model Simulations Using the ECHAM-4 and GISS II Models[a]

PC#1 $\delta^{18}O$	Time Period	Percent of Total Variance Explained	Factor Loadings		
			Huascarán	Quelccaya	Sajama
Ice cores	1976–1984	89.10	0.950	0.935	0.948
Ice cores	1964–1984	81.72	0.891	0.937	0.884
ECHAM-4	1979–1998	71.67	0.744	0.943	0.841
GISS II	1980–1997	79.53	0.838	0.911	0.924

[a]Factor loadings indicate correlation coefficient between PC#1 and individual $\delta^{18}O$ records from Huascarán, Quelccaya, and Sajama.

and the factor loadings (correlation coefficients with the ice core records) of the three PCs based on simulations and observations. The results from the PCA indicate that the three ice core records are very similar and dominated by a common mode of variability over the last 20 years in both observations and simulations. This first mode (PC#1) explains between 80 and 90% of the total variance in the observational record and between 70 and 80% in the simulated records. The factor loadings indicate that all ice cores are highly correlated with this dominant mode. Quelccaya shows factor loadings above 0.9 in both the observed and simulated records, while they are somewhat lower on Sajama and Huascarán, particularly in the ECHAM-4 simulation. Figure 8 shows the correlation of PC#1 based on the simulated and observed ice core records with the NINO3.4 index. Clearly, cold (warm) conditions in the tropical Pacific during the Andean rainy season, on average, will lead to more depleted (enriched) $\delta^{18}O$ values. Even though there are years where this relationship falls apart, both simulated and observed records are significantly correlated with the NINO3.4 index at the 99% confidence level.

5. Discussion and Conclusion

[24] To illustrate the physical link between tropical Pacific climate and related stable isotope variability in Andean ice cores, we correlated the PC#1 time series with contemporaneous (NDJF) tropical SSTA, 200 hPa geopotential height and wind data. SST data were extracted from the Global sea-Ice and Sea Surface Temperature (GISST 2.3a) data set, while 200 hPa geopotential height and wind is based on data from the NCEP-NCAR reanalysis. While Figure 9 shows a correlation coefficient between local SSTA at each grid cell and the reference time series (PC#1), Figure 10 displays a regression coefficient indicating the strength (in gpm or m s^{-1}), sign, and significance of local geopotential height or wind anomalies at each grid cell associated with a unit anomaly of the reference PC#1 time series [e.g., *Garreaud and Aceituno*, 2001].

[25] We further compare our results (plots b–d in Figures 9 and 10) with the typical ENSO pattern by showing a WARM-COLD composite of the respective variables based on SSTA in the NINO3.4 region (plot a in Figures 9 and 10). WARM and COLD episodes are defined as in the work of *Vuille et al.* [2003], that is, the 5-month running mean of SSTA in the NINO3.4 region exceeds (or remains below) 0.5°C (−0.5°C) for at least 6 consecutive months. This comparison enables us to test the hypothesis that it is indeed

the SSTA in the tropical Pacific, which is recorded as the main mode of $\delta^{18}O$ variability on interannual timescales.

[26] The WARM-COLD composite in Figure 9a features the typical ENSO tongue, with positive anomalies centered along the equator and extending from the west coast of South America across the dateline. To the north and south negative anomalies extend from approximately 160°E in a V-shape fashion to 30°N and 30°S. This is consistent with the canonical ENSO mode depicted in many earlier studies based on empirical orthogonal functions [e.g., *Enfield and Mayer*, 1997] or composite SSTA analysis [e.g., *Rasmusson and Carpenter*, 1982]. All correlation fields in Figures 9b–9d are in general agreement with this pattern and thus support the notion of a dominant ENSO-signal in the tropical ice cores, but they also reveal substantial differences between models and observations. While the observational ice core record between 1964 and 1984 shows higher correlations with SSTA over the central equatorial Pacific (Figure 9b), the simulated records based on the ECHAM-4 (1979–1996, Figure 9c) and the GISS II models
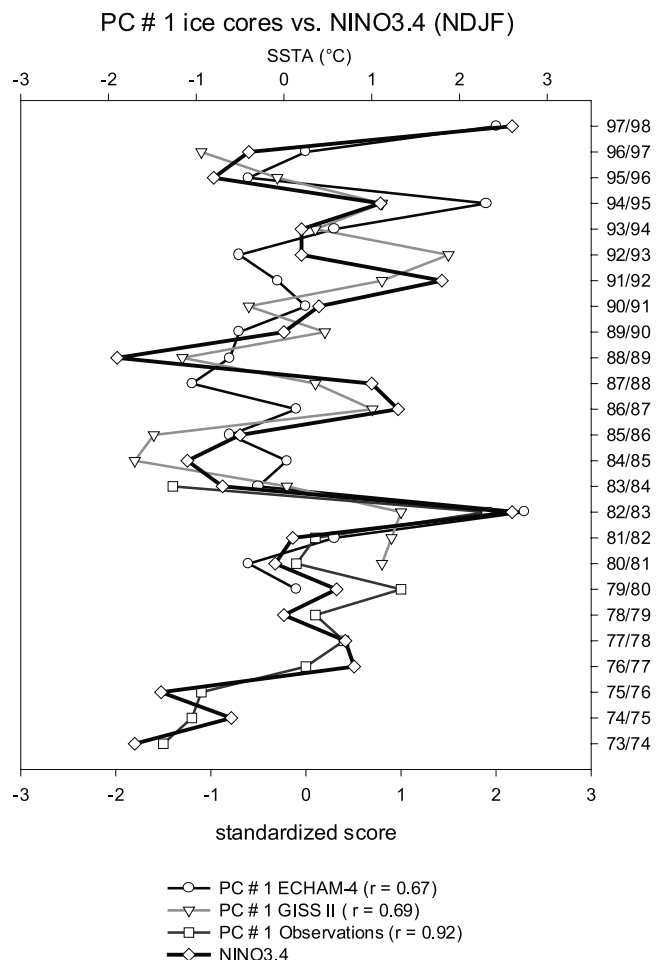
Figure 8. Standardized score time series of PC#1 of $\delta^{18}O$ in precipitation derived from observed and simulated ice core records on Huascarán, Quelccaya, and Sajama plotted against NDJF NINO3.4 index between 1973/1974 and 1997/1998. Correlation coefficient between PC#1 of simulated and observed $\delta^{18}O$ records and NINO3.4 index is indicated in parentheses.
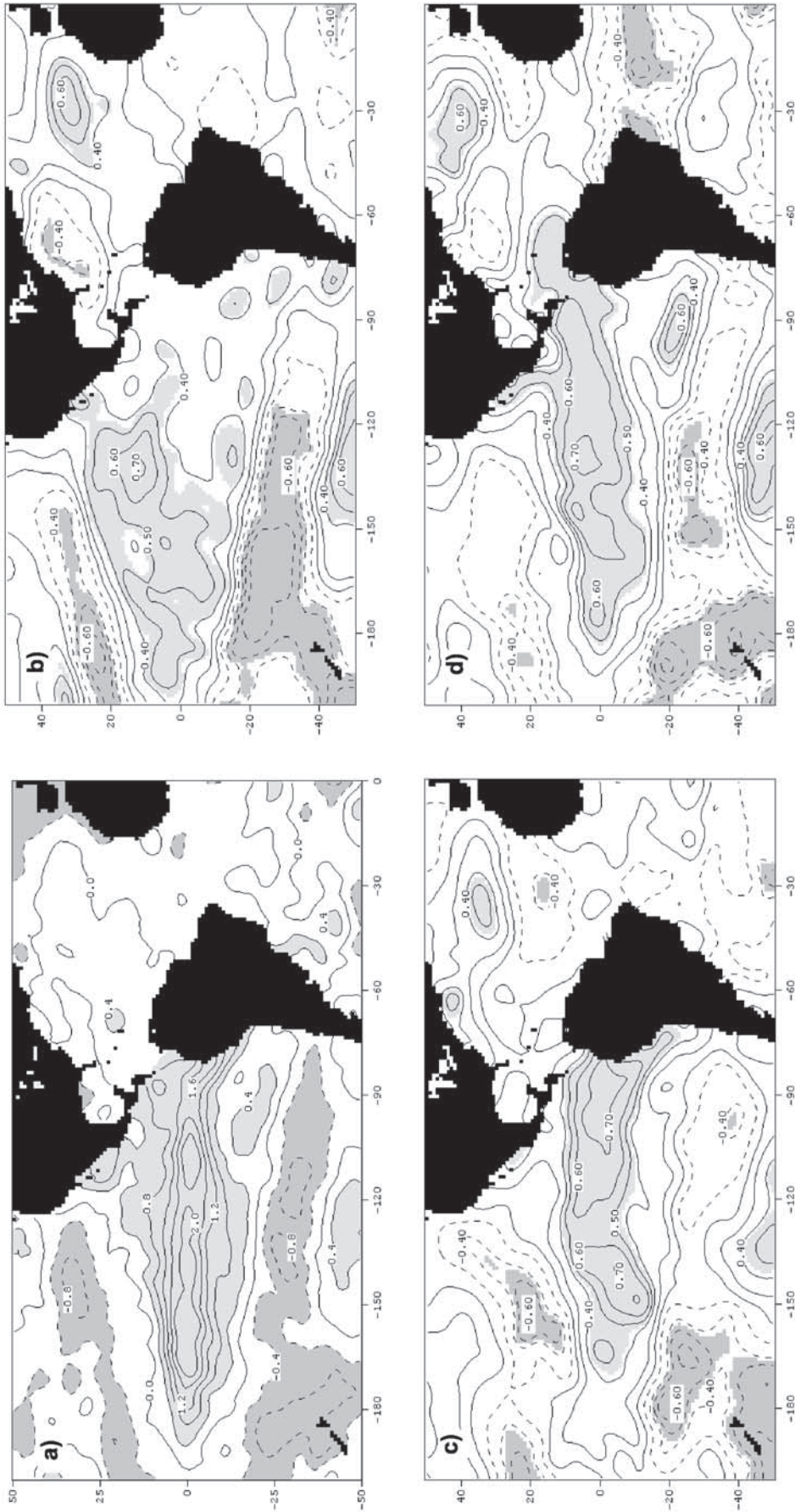
Figure 9. (a) WARM-COLD difference composite (in °C) of NDJF SSTA between 1976 and 1996 with contour interval of 0.4. SST below (above) −0.4 (0.4) shaded in dark (light) gray. (b) Correlation field of PC#1 of δ^{18}O from tropical Andean ice cores with NDJF SSTA based on observations between 1964 and 1984, (c) as in Figure 9b but for ECHAM-4 simulation (1979–1996); (d) as in Figure 9b but for GISS II simulation (1980–1996). Contour interval is 0.2 and 0.1 above 0.4 (below −0.4). Gray shading in Figures 9b, 9c, and 9d indicates significant correlation at the 95% confidence level based on two-tailed Student's *t*-test.
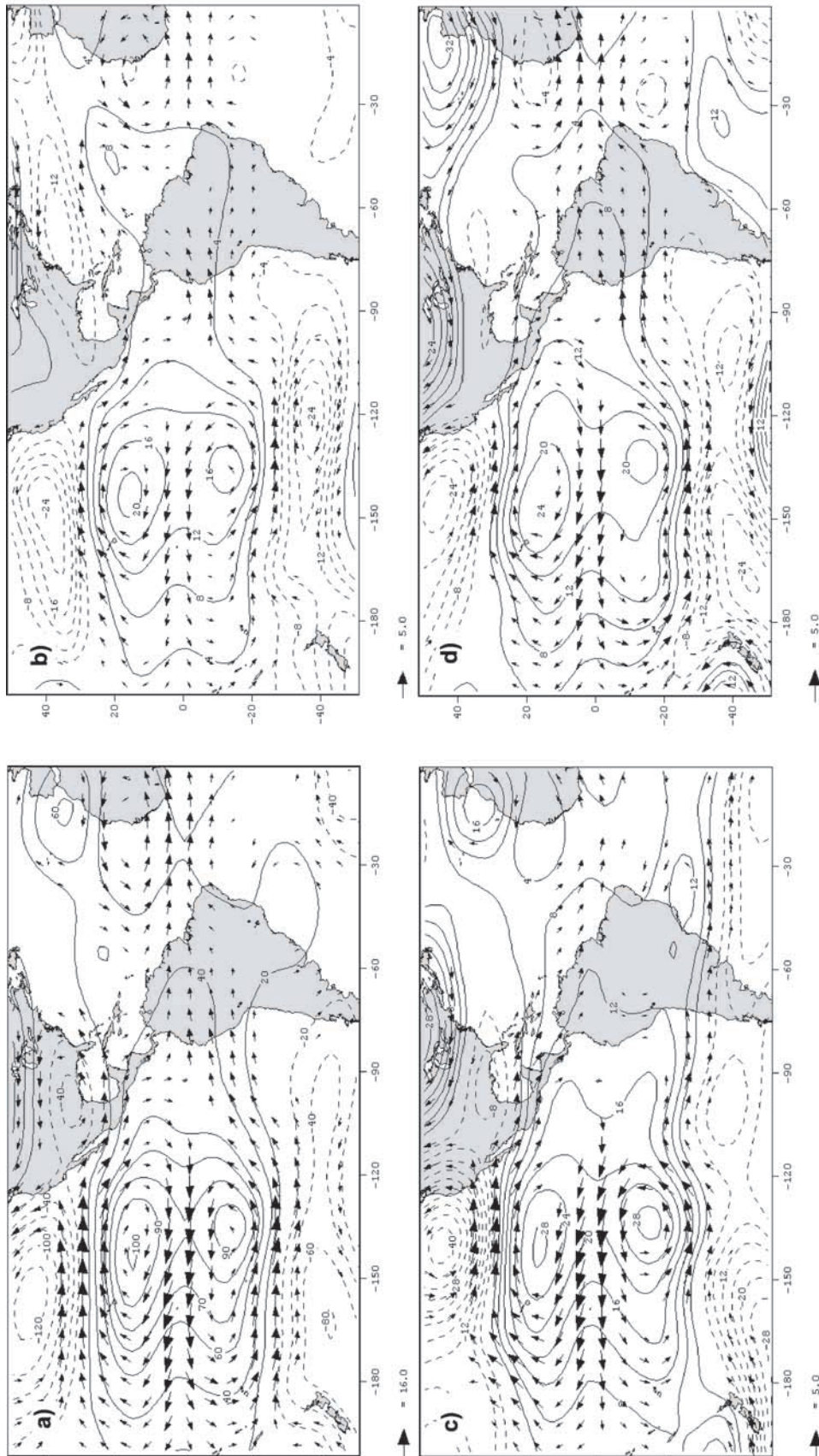
Figure 10. (a) WARM-COLD difference composite of NDJF 200 hPa geopotential height and wind field (1976–1998). Contour interval for geopotential height is 20 and 10 gpm above 60 gpm; negative contours are dashed and zero contour line is omitted. Wind field, with scale (m s^{-1}) indicated on lower left, is only plotted where either zonal or meridional flow is significantly different between WARM and COLD periods at the 95% level, based on two-tailed Student's t-test; (b) PC#1 of δ^{18}O from tropical Andean ice cores regressed upon NDJF 200 hPa geopotential height and wind anomalies (1964–1984); (c) as in Figure 10b but for ECHAM-4 simulation (1979–1998); (d) as in Figure 10b but for GISS II simulation (1980–1997). Contour interval for geopotential height regression coefficient is 4 gpm, negative contours are dashed, and zero contour line is omitted. Wind field, with scale (in m s^{-1}) indicated on lower left, is only plotted where either zonal or meridional flow is significantly correlated with δ^{18}O at the 95% level. Significance levels are based on two tailed Student's t-test.

(1980–1996, Figure 9d) show a closer association with SSTA over the eastern equatorial Pacific. These differences in the correlation fields between simulated and observational data can be attributed to the different time periods used in the correlation analysis and reflect the change in the evolution pattern and the spatial structure of ENSO after the 1976 Pacific climate shift [e.g., *Wallace et al.*, 1998]. If only the data after the Pacific climate shift, 1976–1984, are used in the observational record, the highest correlations are indeed shifted eastward as well (not shown).

[27] In Figure 10a, the WARM-COLD composite of 200 hPa geopotential height and wind is shown. The geopotential height pattern is dominated by the prevalence of positive anomalies throughout the tropics, symmetrical about the equator and a steep meridional geopotential height and temperature gradient along much of the subtropics around 30°N and 30°S, consistent with the notion of a tropical troposphere forced by equatorial Pacific SSTA [e.g., *Yulaeva and Wallace*, 1994; *Wallace et al.*, 1998; *Garreaud and Battisti*, 1999]. Further noteworthy is the distinctive "dumbbell pattern" with anticyclonic rotation about the twin peaks near 140°W at 15°N and 15°S, which is a dynamical response to deep convection over the equatorial Pacific [*Yulaeva and Wallace*, 1994]. All these features are reproduced in the regression fields of both the observed and simulated PC#1 (Figures 10b–10d), thus providing additional evidence for a dominant Pacific control on interannual $\delta^{18}O$ variability in tropical Andean ice cores. It is thus the expansion (shrinkage) of the tropical troposphere associated with a warm (cold) tropical Pacific and the related change in meridional baroclinicity at subtropical latitudes, which leads to enhanced westerly (easterly) flow over the (sub)tropical Andes, apparent in Figure 10. These upper-air wind anomalies, in turn, exert a significant forcing on the low-level moisture flow over the Andes and thus provide the link between oceanic forcing and climate variability on interannual timescales. This mechanism is particularly important over the central Andes, where Sajama and Quelccaya are located [*Garreaud et al.*, 2003].

[28] On the other hand, there is little evidence which would suggest a significant tropical Atlantic influence on $\delta^{18}O$ variability in tropical Andean ice cores, despite the significant correlation with SSTA in parts of the tropical North Atlantic domain (Figures 9b–9d). This region is rather limited in extent and the correlation is not as strong as in the Pacific domain. More importantly, however, SSTA in the Atlantic are only half the size of their tropical Pacific counterparts and are insufficient to force a tropospheric response such as the one observed in Figure 10 [e.g., *Su et al.*, 2001]. The lowlands to the east of the Andes and ultimately the tropical Atlantic are admittedly the moisture source for the precipitation in the tropical Andes. However, while the notion that conditions at the moisture source leave a significant imprint in the $\delta^{18}O$ in a far distant location may be true, one should also take into consideration the fact that atmospheric conditions during transport, as well as climatic conditions at the time of condensation, significantly influence the $\delta^{18}O$ signal as well. All these factors such as atmospheric circulation over the tropical Andes, temperature at the condensation site, convective activity and thus precipitation amount are largely governed by Pacific SSTA on interannual timescales (see review in the work of

Garreaud et al. [2003, and references therein]). If the $\delta^{18}O$ composition indeed reflects tropical Atlantic SSTA, this would imply that at least the $\delta^{18}O$ records from the central Andes (Quelccaya, Illimani, and Sajama) could not be used as a proxy for local climate, because Atlantic SSTA and climate in the central Andes are largely decoupled from each other [*Vuille et al.*, 2000a; *Garreaud et al.*, 2003].

[29] In the past, the $\delta^{18}O$ content in tropical Andean ice cores has been interpreted as a temperature proxy [e.g., *Thompson et al.*, 2000], but more recently also as an indicator of wet or dry conditions in the Andes [*Baker et al.*, 2001]. Our results suggest that these may not necessarily be conflicting views, since in this part of the world precipitation and temperature are strongly correlated on interannual timescales. Both of these two parameters do, however, primarily mirror the oceanic and atmospheric conditions over the tropical Pacific. We therefore interpret the $\delta^{18}O$ in these ice cores as a proxy for tropical Pacific climate. In our view, this is more consistent with the available observational and modeling evidence than trying to disentangle the competing effects of precipitation amount, temperature, and moisture source variability. In this sense, the $\delta^{18}O$ variability recorded in tropical Andean ice cores represents a valuable archive for studying past variability of ENSO [e.g., *Diaz and Pulwarty*, 1994]. Tropical Andean ice cores may thus add to the growing network of paleoarchives, recording Pacific variability on interannual to interdecadal timescales [e.g., *Evans et al.*, 2001], and offer a great prospect, in combination with other proxy records, for unveiling the past climate history of the tropical Pacific region.

References

Aceituno, P., and R. Garreaud, Impacto de los fenomenos el niño y la niña en regimenes fluviometricos andinos, *Rev. Soc. Chilena Ing. Hidraul.*, 10(2), 33–43, 1995.

Aravena, R., O. Suzuki, H. Peña, A. Pollastri, H. Fuenzalida, and A. Grilli, Isotopic composition and origin of the precipitation in Northern Chile, *Appl. Geochem.*, 14, 411–422, 1999.

Baker, P. A., C. A. Rigsby, G. O. Seltzer, S. C. Fritz, T. K. Lowenstein, N. P. Bacher, and C. Veliz, Tropical climate changes at millenial and orbital timescales on the Bolivian Altiplano, *Nature*, 409, 698–701, 2001.

Chaffaut, I., A. Coudrain-Ribstein, J.-L. Michelot, and B. Pouyaud, Précipitations d'altitude du Nord-Chili, origine des sources de vapeur et données isotopiques, *Bull. Inst. Fr. Etud. Andines*, 27, 367–384, 1998.

Charles, C. D., J. Rind, J. Jouzel, R. D. Koster, and R. G. Fairbanks, Glacial-interglacial changes in moisture sources for greenland: Influences on the ice core record of climate, *Science*, 263, 508–511, 1994.

Cole, J. E., D. Rind, R. S. Webb, J. Jouzel, and R. Healy, Climatic controls on interannual variability of precipitation $\delta^{18}O$: Simulated influence of temperature, precipitation amount, and vapor source region, *J. Geophys. Res.*, 104, 14,223–14,235, 1999.

Diaz, H. F., and N. E. Graham, Recent changes in tropical freezing heights and the role of sea surface temperature, *Nature*, 383, 152–155, 1996.

Diaz, H. F., and R. S. Pulwarty, An analysis of the time scales of variability in centuries-long ENSO-sensitive records in the last 1000 years, *Clim. Change*, 26, 317–342, 1994.

Ebbesmeyer, C. C., D. R. Cayan, D. R. McLain, F. H. Nichols, D. H. Peterson, and K. T. Redmond, 1976 Step in the pacific climate: Forty environmental changes between 1968–75 and 1977–1984, in *Proceed-*

ings of the 7th Annual Pacific Climate (PACLIM) Meeting Workshop, April 1990, Interagency Ecol. Stud. Prog. Tech. Rep. 26, edited by J. L. Betancourt and V. L. Tharp, Calif. Dep. of Water Resour., Sacramento, 1991.

Enfield, D. B., and D. A. Mayer, Tropical Atlantic SST variability and its relation to El Niño-Southern Oscillation, J. Geophys. Res., 102, 929–945, 1997.

Evans, M. N., M. A. Cane, D. P. Schrag, A. Kaplan, B. K. Linsley, R. Villalba, and G. M. Wellington, Support for tropically-driven Pacific decadal variability based on paleoproxy evidence, Geophys. Res. Lett., 28, 3689–3692, 2001.

Garcia, M., F. Villalba, L. Araguas-Araguas, and K. Rozanski, The role of atmospheric circulation patterns in controlling the regional distribution of stable isotope contents in precipitation: Preliminary results from two transects in the Ecuadorian Andes, in Isotope Techniques in the Study of Environmental Change, Proc. Ser. IAEA, IAEA-SM-349/7, pp. 127–140, Int. At. Energy Agency, Vienna, 1998.

Garreaud, R., and P. Aceituno, Interannual rainfall variability over the South American Altiplano, J. Clim., 14, 2779–2789, 2001.

Garreaud, R. D., and D. S. Battisti, Interannual (ENSO) and interdecadal (ENSO-like) variability in the southern hemisphere tropospheric circulation, J. Clim., 12, 2113–2123, 1999.

Garreaud, R., M. Vuille, and A. Clement, The climate of the Altiplano: Observed current conditions and mechanisms of past climate change, Palaeogeogr. Palaeoclimatol. Palaeoecol., in press, 2003.

Ginot, P., C. Kull, M. Schwikowski, U. Schotterer, B. Pouyaud, and H. W. Gaeggeler, Effects of post-depositional processes on snow composition of a subtropical glacier (Cerro Tapado, Chilean Andes), J. Geophys. Res., 106, 32,375–32,386, 2001.

Gonfiantini, R., M.-A. Roche, J.-C. Olivry, J.-C. Fontes, and G. M. Zuppi, The altitude effect on the isotopic composition of tropical rains, Chem. Geol., 181, 147–167, 2001.

Grootes, P. M., M. Stuiver, L. G. Thompson, and E. Mosley-Thompson, Oxygen isotope changes in tropical ice, Quelccaya, Peru, J. Geophys. Res., 94, 1187–1194, 1989.

Hardy, D. R., M. Vuille, C. Braun, F. Keimig, and R. S. Bradley, Annual and daily meteorological cycles at high altitude on a tropical mountain, Bull. Am. Meteorol. Soc., 79, 1899–1913, 1998.

Henderson, K. A., L. G. Thompson, and P.-N. Lin, Recording of El Niño in ice core δ^{18}O records from Nevado Huascarán, Peru, J. Geophys. Res., 104, 31,053–31,065, 1999.

Hoffmann, G., and M. Heimann, Water isotope modeling in the Asian monsoon region, Quat. Int., 37, 115–128, 1997.

Hoffmann, G., M. Werner, and M. Heimann, Water isotope module of the ECHAM atmospheric general circulation model: A study on timescales from days to several years, J. Geophys. Res., 103, 16,871–16,896, 1998.

Hoffmann, G., J. Jouzel, and V. Masson, Stable water isotopes in atmospheric general circulation models, Hydrol. Processes, 14, 1385–1406, 2000.

Hoffmann, G., et al., Coherent isotope history of Andean ice cores over the last century, Geophys. Res. Lett., 30, doi:10.1029/2002GL014870, in press, 2002.

Jouzel, J., R. Koster, and S. Joussaume, Climate reconstruction from water isotopes: What do we learn from isotopic models?, NATO Sci. Ser., 1(41), 213–241, 1996.

Jouzel, J., G. Hoffmann, R. D. Koster, and V. Masson, Water isotopes in precipitation: Data/model comparison for present-day and past climates, Quat. Sci. Rev., 19, 363–379, 2000.

Kalnay, E., et al., The NCEP/NCAR 40-year reanalysis project, Bull. Am. Meteorol. Soc., 77, 437–471, 1996.

Krinner, G., C. Genthon, and J. Jouzel, GCM analysis of local influences on ice core delta signals, Geophys. Res. Lett., 24, 2825–2828, 1997.

Melice, J. L., and P. Roucou, Decadal time scale variability recorded in the Quelccaya summit ice core δ^{18}O isotopic ratio series and its relation with sea surface temperature, Clim. Dyn., 14, 117–132, 1998.

Pierrehumbert, R. T., Huascaran δ^{18}O as an indicator of tropical climate during the last glacial maximum, Geophys. Res. Lett., 26, 1345–1348, 1999.

Rasmusson, E. M., and T. H. Carpenter, Variations in tropical sea surface temperature and surface wind fields associated with the Southern Oscillation/El Niño, Mon. Weather Rev., 110, 354–384, 1982.

Rind, D., and D. Peteet, Terrestrial conditions at the last glacial maximum and CLIMAP sea-surface temperature estimates: Are they consistent?, Quat. Res., 24, 1–22, 1985.

Steig, E. J., P. M. Grootes, and M. Stuiver, Seasonal precipitation timing and ice core records, Science, 266, 1885–1864, 1994.

Stephens, C., S. Levitus, J. Antonov, and T. P. Boyer, On the Pacific Ocean regime shift, Geophys. Res. Lett., 28, 3721–3724, 2001.

Stichler, W., U. Schotterer, K. Froehlich, P. Ginot, C. Kull, H. W. Gaeggeler, and B. Pouyaud, The influence of sublimation on stable isotope

records recovered from high altitude glaciers in the tropical Andes, J. Geophys. Res., 106, 22,613–22,620, 2001.

Su, H., D. Neelin, and C. Chou, Tropical teleconnection and local response to SST anomalies during the 1997–1998 El Niño, J. Geophys. Res., 106, 20,025–20,043, 2001.

Thompson, L. G., Reconstructing the paleo ENSO records from tropical and subtropical ice cores, Bull. Inst. Fr. Etud. Andines, 22, 65–83, 1993.

Thompson, L., E. Mosley-Thompson, and B. J. Arnao, El Niño-Southern Oscillation events recorded in the stratigraphy of the tropical Quelccaya ice cap, Peru, Science, 226, 50–52, 1984.

Thompson, L. G., E. Mosley-Thompson, J. F. Bolzan, and B. R. Koci, A 1500 year record of tropical precipitation in ice cores from the Quelccaya ice cap, Peru, Science, 229, 971–973, 1985.

Thompson, L. G., E. Mosley-Thompson, M. Davis, P. N. Lin, T. Yao, M. Dyurgerov, and J. Dai, Recent warming: Ice core evidence from tropical ice cores with emphasis on Central Asia, Global Planet. Change, 7, 145–156, 1993.

Thompson, L. G., E. Mosley-Thompson, M. E. Davis, P.-N. Lin, K. A. Henderson, J. Cole-Dai, J. F. Bolzan, and K.-B. Liu, Late glacial stage and holocene tropical ice core records from Huascaran, Peru, Science, 269, 46–50, 1995.

Thompson, L. G., et al., A 25,000-year tropical climate history from Bolivian ice cores, Science, 282, 1858–1864, 1998.

Thompson, L. G., E. Mosley-Thompson, and K. Henderson, Ice-core palaeoclimate records in tropical South America since the last glacial maximum, J. Quat. Sci., 15, 377–394, 2000.

Von Storch, H., and F. W. Zwiers, Statistical Analysis in Climate Research, 484 pp., Cambridge Univ. Press, New York, 1999.

Vuille, M., Atmospheric circulation over the Bolivian Altiplano during dry and wet periods and extreme phases of the Southern Oscillation, Int. J. Climatol., 19, 1579–1600, 1999.

Vuille, M., D. R. Hardy, C. Braun, F. Keimig, and R. S. Bradley, Atmospheric circulation anomalies associated with 1996/1997 summer precipitation events on Sajama ice cap, Bolivia, J. Geophys. Res., 103, 11,191–11,204, 1998.

Vuille, M., R. S. Bradley, and F. Keimig, Interannual climate variability in the Central Andes and its relation to tropical Pacific and Atlantic forcing, J. Geophys. Res., 105, 12,447–12,460, 2000a.

Vuille, M., R. S. Bradley, and F. Keimig, Climatic variability in the Andes of Ecuador and its relation to tropical pacific and Atlantic sea surface temperature anomalies, J. Clim., 13, 2520–2535, 2000b.

Vuille, M., R. S. Bradley, M. Werner, R. Healy, and F. Keimig, Modeling δ^{18}O in precipitation over the tropical Americas, 1, Interannual variability and climatic controls, J. Geophys. Res., 108, doi:10.1029/2001JD002038, in press, 2003.

Wagnon, P., F. Vimeux, H. Bonnaveira, E. Berthier, M. de Angelis, and J. R. Petit, Influence of snow surface sublimation on stable isotope and chemical records and on surface energy balance over a Bolivian glacier, Illimani, Eos Trans, AGU, 82(47), Fall Meet. Suppl., F549, 2001.

Wallace, J. M., E. M. Rasmusson, T. P. Mitchell, V. E. Kousky, E. S. Sarachik, and H. von Storch, On the structure and evolution of ENSO related climate variability in the tropical Pacific: Lessons from TOGA, J. Geophys. Res., 103, 14,241–14,259, 1998.

Werner, M., and M. Heimann, Modeling interannual variability of water isotopes in Greenland and Antarctica, J. Geophys. Res., 107(D1), 4001, doi:10.1029/2001JD900253, 2002.

Werner, M., U. Mikolajewicz, M. Heimann, and G. Hoffmann, Borehole versus isotope temperatures on Greenland: Seasonality does matter, Geophys. Res. Lett., 27, 723–726, 2000.

Werner, M., M. Heimann, and G. Hoffmann, Isotopic composition and origin of polar precipitation in present and glacial climate simulations, Tellus, Ser. B, 53, 53–71, 2001.

Yulaeva, E., and J. M. Wallace, The signature of ENSO in global temperature and precipitation fields derived from the microwave sounding unit, J. Clim., 7, 1719–1736, 1994.

————————————

R. S. Bradley, D. R. Hardy, F. Keimig, and M. Vuille, Climate System Research Center, Department of Geosciences, Morrill Science Center, University of Massachusetts, 611 North Pleasant Street, Amherst, MA 01003-9297, USA. (rbradley@geo.umass.edu; dhardy@geo.umass.edu; frank@geo.umass.edu; mathias@geo.umass.edu)

R. Healy, Woods Hole Oceanographic Institution, M.S. 8, 360 Woods Hole Road, Woods Hole, MA 02543, USA. (rhealy@whoi.edu)

L. G. Thompson, Byrd Polar Research Center, Ohio State University, 108 Scott Hall, 1090 Carmack Road, Columbus, OH 43210, USA. (thompson.3@osu.edu)

M. Werner, Max Planck Institute for Biogeochemistry, P. O. Box 10 01 64, D-07701 Jena, Germany. (martin.werner@bgc-jena.mpg.de)